Polymer Degradation and Stability 232 (2025) 111128

Contents lists available at ScienceDirect

Polymer Degradation and Stability

journal homepage: www.journals.elsevier.com/polymer-degradation-and-stability

Defining the degree of degradation in plastics: Quantification of accumulated degradation products and leached stabilizers for predicting end-of-life

Yusuke Hibi [a,*], Tsukasa Matsumoto [b], Masatoshi Midorikawa [c], Shiho Uesaka [a], Makoto Mizoshiri [b], Toshiyuki Tanimura [b], Masato Okada [b], Kimiyoshi Naito [c,*], Masanobu Naito [a,*]

[a] Data-driven Polymer Design Group, Research Center for Macromolecules and Biomaterials, National Institute for Materials Science (NIMS), 1-2-1, Sengen, Tsukuba, Ibaraki 305-0047, Japan
[b] Dai Nippon Printing Co., Ltd., 1-1-3 Midorigahara, Tsukuba, Ibaraki, 300-2646, Japan
[c] Polymer Matrix Composites Group, Materials Manufacturing Field, Research Center for Structural Materials, National Institute for Materials Science, Tsukuba 305-0047, Japan

ARTICLE INFO

Keywords:
Degradation metrics
Beyond carbonyl index
Microplastics
Additive leaching
Pyrolysis mass spectrometry

ABSTRACT

Plastics degrade through various mechanisms, complicating the comprehensive chemical definition of degradation. As the accumulation of degraded products leads to sudden declines in material properties and triggers microplastic dispersion, a chemical degradation metric is essential for predicting plastics' end-of-life. Here, we propose defining degradation by the weight ratio of "completely degraded polymer (CDP)" to pristine polymer, determined via pyrolysis mass spectrometry (MS). By simplifying the complex degradation evaluation into a straightforward framework of compositional analysis, a comprehensive degradation metric can be obtained without tracking individual degradation pathways. Moreover, by including stabilizers as system components, stabilizer leaching and polymer degradation can be concurrently visualized in the same framework. We demonstrate this approach in polyurethane films subjected to accelerated degradation tests and, by correlating the CDP-defined degradation metric with mechanical property evaluations, successfully identify the threshold degradation level that marks a material's end-of-life. Furthermore, this method reveals deeper insights into degradation mechanisms: stabilizer leaching and polymer degradation are complementary processes that induce each other. This comprehensive degradation metric will also be crucial for grading recycled materials, promoting the circular economy in plastics.

1. Introduction

Plastics deteriorate and eventually fail. Detecting early signs of this degradation is crucial for maintaining aging infrastructure and preventing the release of microplastics [1,2]. However, polymers degrade through various pathways, including chemical changes in repeating unit structures, main chain scission, oxidation, crosslinking, and leaching of stabilizers [3–5]. This complexity makes it difficult to establish a comprehensive chemical metric for assessing degradation, complicating efforts to determine the material's remaining lifespan. Identifying when degradation accelerates microplastic release is critical for addressing plastic pollution [6,7]. Furthermore, establishing a standardized evaluation method for degradation is essential for grading recycled materials [8]. This is particularly relevant in the emerging circular economy models [9], where the choice between material and chemical recycling depends on the extent of degradation. When degradation is minimal, material recycling offers a more energy-efficient solution. In contrast, advanced degradation requires chemical recycling to break down polymers into monomers, requiring more energy. A reliable method for quantifying degradation supports better decisions, balancing recycled material quality and energy efficiency.

According to IUPAC, polymer degradation is defined as "chemical changes in a polymeric material that usually result in undesirable changes in the in-use properties of the material" [10]. On the other

* Corresponding authors.
E-mail addresses: hibi.yusuke@nims.go.jp (Y. Hibi), naito.kimiyoshi@nims.go.jp (K. Naito), naito.masanobu@nims.go.jp (M. Naito).

https://doi.org/10.1016/j.polymdegradstab.2024.111128
Received 30 October 2024; Received in revised form 2 December 2024; Accepted 5 December 2024
Available online 6 December 2024

hand, polymer decomposition is distinguished from polymer degradation which refers to the breakdown of polymers into smaller structures. Thus, polymer degradation is a broader concept that encompasses polymer decomposition. Considering a more inclusive degradation degree is essential for understanding the property deterioration of polymeric materials. In the absence of a comprehensive chemical definition of degradation degree [11], physical property changes often serve as an alternative measure. However, the relationship between physical properties and the accumulation of degraded products is often nonlinear. Mechanical strength may remain stable until a critical threshold of degraded products is reached, after which it declines rapidly. This makes it difficult to predict sudden material failure based solely on physical metrics. Integrating chemical compositional analysis is therefore essential to chemically identify this threshold. This deeper insight helps in developing durable materials and provides a more accurate and standardized metric for degradation, guiding recycling strategies.

A common chemical metric is the carbonyl index (CI), which detects carbonyl groups formed by oxidation using infrared spectroscopy (IR) [7]. However, CI has limitations, particularly when the polymer contains inherent carbonyl groups, and it does not account for other degradation mechanisms not involving carbonyl addition [11]. Techniques like nuclear magnetic resonance [12], size-exclusion chromatography [13] and X-ray photoelectron spectroscopy [14] can complement CI to address other pathways. However, selecting the appropriate technique is challenging without prior knowledge of the degradation mode, and no method has been established to quantitatively assess the degree of degradation when multiple modes occur simultaneously.

To capture all degradation behaviors without identifying the specific degradation mechanism, we propose defining the degree of degradation by the weight ratio of "completely degraded polymer (CDP)" to pristine polymer using quantitative pyrolysis mass spectrometry (pyrolysis-MS) [15–17]. CDP here refers to a hypothetical state reached by the polymer material after prolonged environmental exposure. By simplifying the complex degradation evaluation into a straightforward compositional analysis, we would obtain a comprehensive degradation metric without monitoring individual degradation pathways. It also allows for the visualization of stabilizer leaching within the same framework.

While our method does not rely on prior knowledge of specific degradation mechanisms, alternative approaches, such as targeting specific reference molecules via pyrolysis-gas chromatography-MS [18], may be effective for systems where degradation pathways are well understood. Quantifying changes in marker molecules between pristine and degraded polymers can be valuable in working environments where degradation products are fully characterized. In contrast, our approach captures the total spectral modulation associated with degradation, offering a broader and more inclusive metric applicable to diverse polymers and degradation conditions.

We validate this method using polyurethane films subjected to accelerated degradation tests, aiming to identify the degradation threshold that triggers sudden declines in mechanical properties. Additionally, we monitor the reduction in mechanically connected domain size, which indicates decreasing internal cohesion and leads to microplastic dispersal.

2. Materials and methods

2.1. Film preparation

UV-cured polyurethane oligomer (ShikohUV-6630B; Mitsubishi Chemicals), photo-initiator of Omnirad 184 (4 wt%) and specified amounts of hindered amine light stabilizers (HALS; Tinuvin 123, BASF) and/or ultraviolet absorber (UVA; Tinuvin 400, BASF) were premixed and applicator-coated onto a polyethylene terephthalate substrate (Toyobo A4160) with thickness of 0.05 mm. The film was then cross-linked by UV irradiation (Excelitas Noblelight Japan; wavelength range: 200~450 nm; irradiation dose: 0.98 J/cm^2 at 365 nm). After UV irradiation, the film was peeled off the substrate to form a freestanding film, which was then subjected to accelerated degradation tests.

2.2. Accelerated degradation test

The polyurethane freestanding film was attached to an accelerated weathering tester (DAIPLA WINTES; KW-R7TP-A) using tape. The accelerated degradation test was performed by alternating between UV exposure and humidification. UV exposure (using a metal halide lamp; irradiation dose: 65 mW/cm^2 at 365 nm) was conducted for 20 h, followed by 4 h of humidification at 30 °C with a relative humidity of 98 %. During UV exposure, to account for the temperature increase due to UV absorption, conditions were controlled to maintain a black panel temperature of 63 °C and a relative humidity of 50 %. This 24-hour cycle of 20 h of UV exposure and 4 h of humidification was repeated for 0, 3, 7, 14, 30, and 60 days. According to a literature [19], calculations based on UV exposure suggest that 60 days of accelerated degradation is equivalent to 25 years of degradation in an outdoor environment. After the predetermined degradation durations, the films were allowed to air dry indoors and was then subjected to IR, pyrolysis-MS, and physical property testing.

2.3. IR measurements

IR measurements were conducted using Nicolet Summit (Thermo Fisher Scientific) with attenuated total reflection (ATR) method. After accelerated degradation, an ATR prism (diamond crystal) was pressed against either the UV-exposed surface (top surface) or the substrate side (back surface) of the samples. The cosine similarity of the IR spectra was calculated in the range of 650 – 4000 cm^{-1} using the standard procedure, which involves taking the dot product of the L2-normalized spectra of pristine and degraded films.

2.4. Pyrolysis-MS measurements

Pyrolysis-MS were conducted using a connected system of thermogravimetry (TG-DTA8122; Rigaku) and mass spectrometry (JMS-T2000GC AccuTOF; JEOL) with electron impact (EI) ion source (20 eV). The film samples were punched out with a diameter of 4 mm and placed in the bottom of double-bottom aluminum pans. As an internal standard, di-*tert*-butyl biphenyl was placed in the upper section of the double-bottom pans. The temperature was increased at a rate of 25 °C/min, and data were collected between 250 °C and 550 °C. The sample quantities were calculated based on the weight loss rate from thermogravimetry. MS data were centroided using msAxel (JEOL) and input into the previously reported TG-synchronized NL-RQMS algorithm. The detailed procedures are described in the Supporting Information and previous report [17].

2.5. Micro-indentation

The degraded film was adhered onto SUS329 substrates using cyanoacrylate adhesive (TOAGOSEI; Aron Alpha). To ensure the film adhered to the substrate with a constant force, a release film was placed over the sample film, then SUS329 was placed on top to create a sandwich with the substrate. This assembly was clamped with clips and left overnight. Micro indentation tests were conducted using a dynamic ultra micro hardness tester (Shimadzu; DUH-211S) with an indenter (115° triangular pyramid; modulus: 1.14×10^6 MPa; Poisson's ratio: 0.07) in loading-unloading mode (applied maximum force: 50 mN, loading and unloading time: 5 s). The calculations for indentation modulus were conducted from the slope of unloading curves in the range of 70–20 % force.

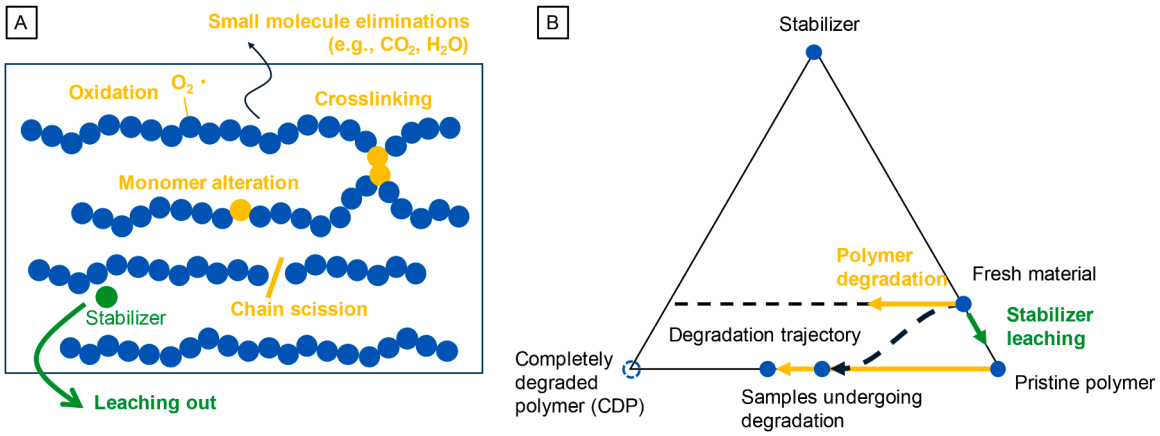

Fig. 1. Chemical and quantitative definition of degradation degree. (A) Various degradation modes in polymer materials. In addition to the illustrated pathways, isomerization/tautomerization may occur in polymers with double bonds in the main chain or in stereospecific polymers, leading to structural rearrangements. (B) Visualization of degradation in a ternary plot of pristine polymer, stabilizer, and CDP. The degradation degree of the samples is defined by the ratio of the distances from the sample to the pristine polymer and CDP vertices.

2.6. SAICAS

The same films adhered onto SUS used for micro-indentation tests were reused for SAICAS (DAIPLA WINTES; SAICAS EN-type). The films were first scored to create narrow strips with width of about 0.7 mm using side cutter (DAIPLA WINTES). The SAICAS cutting process was performed using a ceramic blade with a horizontal speed of 5 μm and a vertical speed of 0.5 μm. After reaching a depth of 25 μm, the process was switched to horizontal movement, and the horizontal load was recorded.

3. Results and discussion

3.1. Definition of degradation degree using pyrolysis-MS

As shown in Fig. 1A, plastics degrade through multiple pathways depending on specific operational environments. The extent of this degradation can be captured as the CDP fraction, while stabilizer leaching is quantified by measuring the remaining stabilizer content in the sample. Both polymer degradation and stabilizer leaching can thus be visualized using the ternary composition diagram in Fig. 1B. As plastics often contain stabilizers, the starting point lies along the edge between the pristine polymer and stabilizer vertices. Leftward movement represents polymer degradation, while downward movement indicates stabilizer leaching. Since these processes typically occur simultaneously, plotting the degradation trajectory on the ternary diagram provides a comprehensive and quantitative view of degradation from a chemical composition perspective. By correlating this chemical degradation degree with changes in mechanical strength analyzed by micro-indentation tests[20] and surface and interfacial cutting analysis system (SAICAS)[21], the degradation threshold that triggers sudden declines in properties and microplastic formation can be identified.

The chemical compositional analysis must be performed using a highly sensitive analytical technique capable of detecting various degradation modes and tracking changes in the content of stabilizers, even in trace amounts. Additionally, because many plastic materials are insoluble due to crosslinking, a method capable of directly measuring solid materials is desirable. Pyrolysis-MS meets all of these requirements and stands as an optimal candidate. In pyrolysis-MS, polymer materials are gradually heated, and the masses of the evolved gases are continuously analyzed, yielding a 2D spectrum with mass-to-charge ratio (m/z) and temperature axes with rich polymer information. [22–24] It also excels in trace detection at the 1000 ppm level [16], allowing for accurate evaluation of decreasing stabilizer by leaching. These characteristics make pyrolysis-MS a comprehensive analytical technique for capturing various degradation behaviors.

By deconvoluting the analyte spectrum into reference spectra of pristine polymers, stabilizer and CDP, the degradation degree and stabilizer residual amount can be determined. However, CDP is a hypothetical entity within a realistic timeframe, and therefore, its reference spectrum cannot be directly measured. To address this issue, we inferred the spectrum of CDP based on partially degraded polymers prepared via accelerated degradation tests for several weeks. These samples can be considered as mixtures of CDP and pristine polymer at certain mixing ratios, depending on their degree of degradation. The inference of missing reference spectra from observed mixture spectra has been well-established in the reference-free quantitative MS (RQMS) framework [15–17]. As stabilizers such as radical scavengers may alter polymer thermal degradation behavior, accounting for nonlinear stabilizer–polymer interaction is necessary. We therefore employed nonlinear (NL-) RQMS algorithm, recently developed by Hibi [17], to address this nonlinear spectral distortion.

Since the reference spectra of pristine polymer and stabilizers are directly measurable, inferring the CDP spectrum would complete the reference set to draw the compositional triangle diagram of pristine polymer–stabilizers–CDP, which can visualize comprehensive degradation behaviors. We validated this concept in cross-linked polyurethane films containing hindered amine light stabilizers (HALS), which were subjected to accelerated degradation test simulating outdoor environments with rain and sun light. Polyurethane is frequently used as a top-coated protective layer due to its excellent abrasion and scratch resistance [25,26]. Since it is at the forefront of degradation resistance, understanding its degradation behavior and the leaching of stabilizers is particularly meaningful. However, the proposed method did not rely on any assumptions specific to polyurethane and can be applied to various polymers.

3.2. Verification of the existence of completely degraded polymer (CDP)

To begin with, we verified the validity of assuming the existence of the hypothetical entity CDP. If the degrading polymers eventually converge into CDP after a sufficiently long weathering period, chemical changes due to degradation should gradually decrease, which is known to be true for most polymer species [3]. To experimentally confirm this assumption, polyurethane films without stabilizers were subjected to accelerated degradation tests for up to 60 days—suggested to be roughly corresponding to 25 years in an outdoor natural environment[19]—and the temporal evolution of their IR spectra was observed. The test films

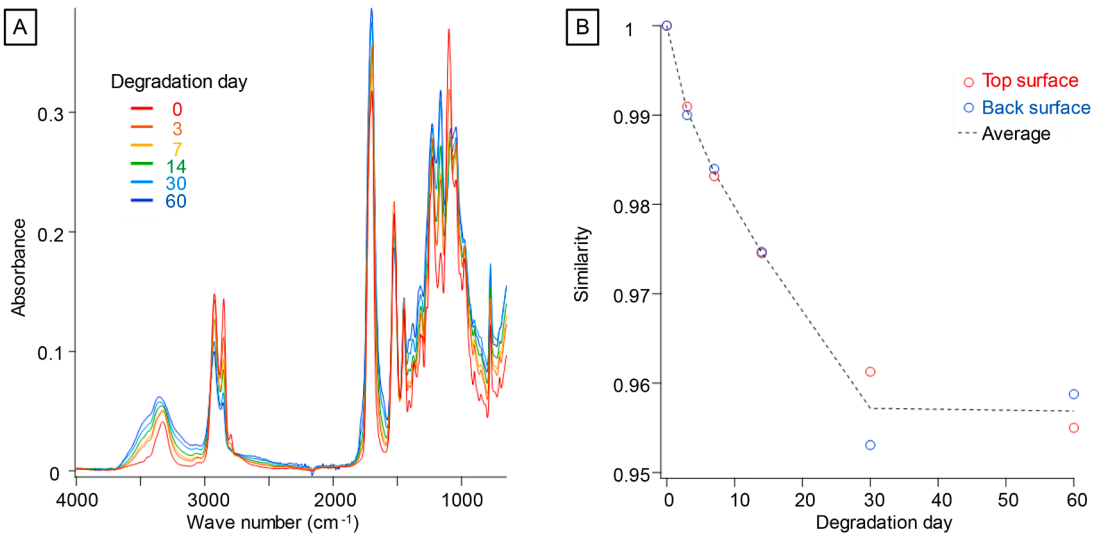

Fig. 2. IR spectra of polyurethane films subjected to accelerated degradation tests. (A) Temporal evolution of ATR-IR spectra on top surfaces of the films. (B) Cosine similarities of IR spectra of degraded films on top (red) and back (blue) surfaces. The dot curve represents the averaged similarity of top and back surfaces.

were sufficiently thick (50 μm) to be self-supporting, allowing for analysis of chemical information on the top and back surfaces via the ATR method. As seen in Fig. 2A, degradation caused some changes in the IR spectra; however, the spectra at 30 and 60 days were almost consistent, as indicated by the overlapping teal and blue curves.

To quantitatively understand the convergence, we introduced a metric of cosine similarity based on the pristine spectrum. This metric takes a value between 0 and 1 in non-negative spectroscopies, indicating the similarity between two spectra. A value closer to 1 indicates that the spectrum of the degraded sample closely matches that of the pristine polymer. Fig. 2B shows that the spectral similarity decreased to 0.95, but the variation converged after 30 days of degradation on both top and bottom surfaces. The slowing of the variation suggested the existence of the ultimate limitation of degradation, which we call CDP. The slowing is primarily attributed to the depletion of reactive chemical species. However, an additional possibility is that oxygen diffusion into the polymer's interior may have slowed due to the formation of a degraded surface layer acting as a protective barrier. Regardless of the underlying mechanism, once the degradation reactions have slowed down significantly, it is reasonable to consider that the polymer has reached a state equivalent to CDP in the working environment of interest. The cosine similarity in IR spectra was effective for evaluating various degradation modes quantitatively and comprehensively. However, the calculation of cosine similarity assumes that all peak changes are equally significant. This assumption is inappropriate, as in IR spectroscopy the peak intensity ratio is not proportional to the abundance ratio of the corresponding substructures. Furthermore, the high cosine similarity of 0.95 between the pristine and long-term degraded polymers indicated that the changes in IR spectra induced by degradation were not significant. Therefore, performing highly sensitive degradation assessments using IR was challenging. Moreover, IR was not suitable for detecting trace additives, as suggested by the nearly identical spectra of polyurethanes with or without 3 wt% of HALS (Fig. S1), which prevented the evaluation of stabilizer leaching. However, based on the verified assumption of

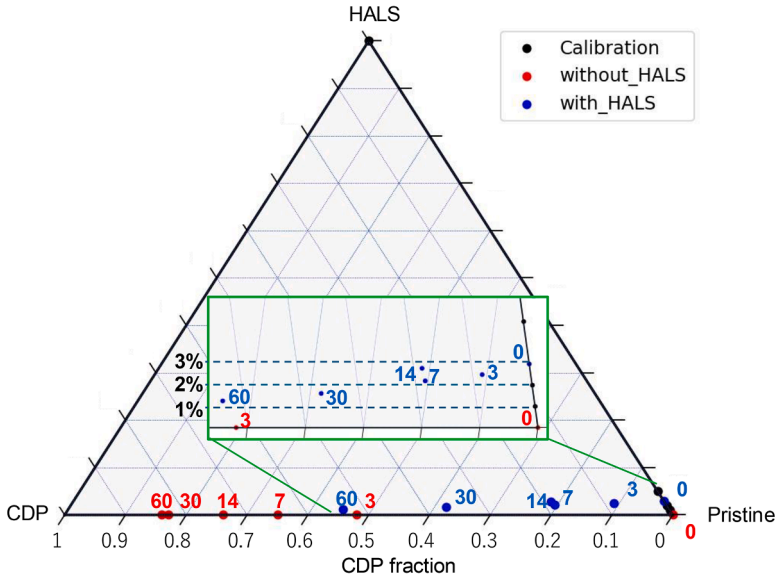

Fig. 3. Compositional ternary diagram of the pristine polymer–HALS–CDP system analyzed by NL-RQMS. The numbers indicate the exposure days in accelerated degradation test. Blue and red dots represent the accelerated degradation samples with and without 3 wt% additive of HALS. Black dots on the pristine–HALS edge are the calibration samples with known amounts of HALS (100 wt%, 5 wt%, 2 wt%, 1 wt%). The inset shows a magnified region related to HALS leaching.

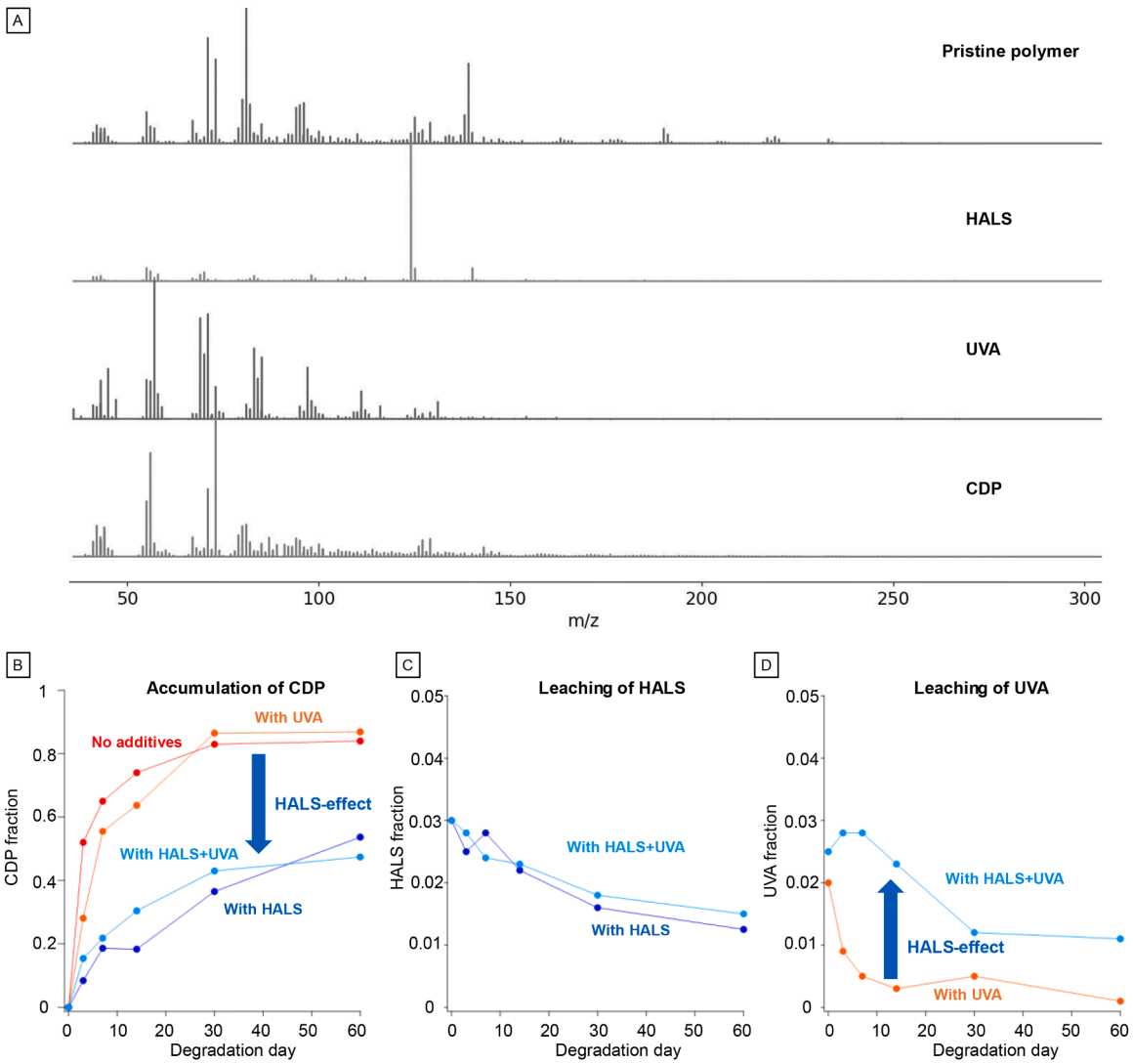

Fig. 4. Stabilizer effects and leaching in polymer degradation. (A) Reference spectra of the quaternary system consisting of pristine polymer, HALS, UVA, and CDP. The CDP spectrum was inferred by NL-RQMS. (B) Accumulation of the CDP fraction along with the progression of degradation. The red, orange, blue, and teal curves represent four types of films with no stabilizers, UVA, HALS, and both of UVA and HALS, respectively. (C) Amount of residual HALS in the films containing HALS (blue) and HALS+UVA (teal) (D) Amount of residual UVA in the films containing UVA (orange) and HALS+UVA (teal).

CDP existence, degradation assessment by pyrolysis-MS overcame all these drawbacks, as we will demonstrate in the next section.

3.3. *Visualization of degradation behavior via pyrolysis-MS*

IR analysis revealed that degradation slowed down, suggesting the existence of CDP. However, 60 days of accelerated degradation may not be sufficient to reach the ultimate degradation limit, and the theoretical CDP cannot be prepared within a fixed timescale. Nevertheless, NL-RQMS can infer this missing reference using CDP–pristine mixtures obtained from degradation tests, even in the presence of component interactions. [17] To this end, a dataset consisting of two series of degraded samples with various degradation durations, both with and without HALS, was input into the NL-RQMS (all used raw spectra and sample information are attached as Data S1. The used algorithm is presented in the literature[17]). The dataset also included samples with various amounts of HALS at 100 wt%, 5 wt%, 2 wt%, and 1 wt% that were not subjected to degradation tests, for calibrating HALS fraction. The result is depicted as ternary diagram in Fig. 3. Significantly, in the ternary diagram, the samples with longer degradation duration were located on the left side closer to the CDP vertex, although the information about degradation duration was not input into NL-RQMS algorithm. This clearly suggest the accurate inference of CDP spectrum (presented in Fig. 4A), and correctly captured the trend of the increments of CDP fraction along with increased degradation duration. Another important point is that the progression of degradation was significantly suppressed in the HALS-added system (blue dots) compared to the system without HALS (red dots); the degree of degradation of the sample with HALS after 60 days degradation corresponds to that of the sample without HALS after only three days. This allows for the quantitative evaluation of the effectiveness of stabilizers. Furthermore, HALS-containing system shifted towards the bottom left, approaching the CDP-pristine edge as the degradation days increase (see the inset in Fig. 3). This indicated that the amount of HALS decreased from 3 wt% to approximately 1 wt% after 60 days of degradation. Overall, NL-RQMS analysis allowed for the quantitative assessment of degradation levels, stabilizer effectiveness, and stabilizer leaching, providing a comprehensive understanding of degradation behavior.

3.4. *Stabilizer effects on degradation behaviors*

In practice, multiple stabilizers are often used together, complicating

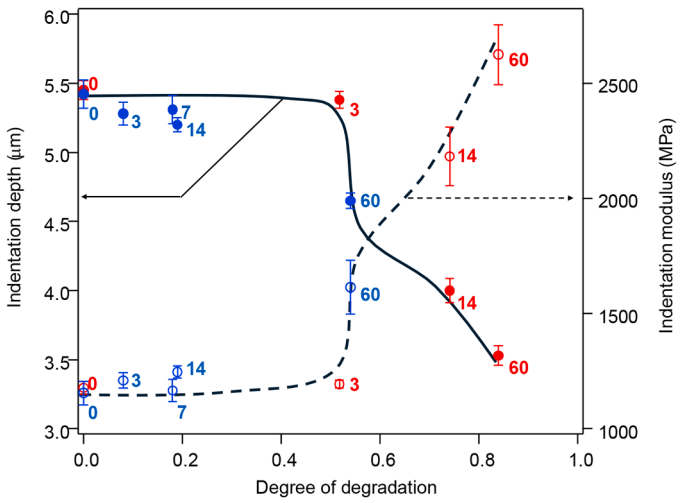

Fig. 5. Micro-indentation test. The indentation depth (closed circles) and indentation modulus (open circles) are shown for HALS-containing films (blue) and non-HALS-containing films (red). The numbers indicate the degradation duration. For each film, 10 different points were indented, and the averaged values for both indentation depth and modulus are plotted. The error bars represent standard deviations for the 10 attempts. The curves were hand-drawn as a guide to illustrate the sequential changes in mechanical properties over the course of degradation.

the system further. To examine whether NL-RQMS can independently detect the leaching of several stabilizers, we analyzed the degradation of a quaternary system consisting of pristine polymer, HALS, UVA, and CDP, with reference spectra shown in Fig. 4A. This series of experiments would allow for a quantitative comparison of the degradation inhibition capabilities of HALS and UVA in polymers. The inferred CDP spectrum differs significantly from that of the pristine polymer, and a focused investigation of the spectral changes between these two could reveal the specific degradation reactions occurring (also see the internal processed data from NL-RQMS in Fig. S2). However, pyrolysis-MS often produces complex peak patterns due to uncontrolled pyrolysis, making prior knowledge of the chemical structure of pristine materials essential for interpreting the spectral changes chemically. Unfortunately, much of this information for practical polymer materials is proprietary and undisclosed. The polyurethane oligomer used in this study was no exception; its structural formula was not publicly available. Without detailed reverse engineering, deducing the structure and its degradation-induced changes solely from the pyrolysis-MS of the cross-linked polymer was challenging. Nevertheless, even without such information, NL-RQMS offers the advantage of accurately quantifying the composition of degradation products and residual stabilizers while accounting for their interactions [17]. This capability highlights its value as a practical analytical technique: regardless of the polymer's structure or working environment, CDP-defining degradation metrics can be derived solely from the MS spectral data. Fig. 4B shows CDP accumulation in four types of films: one with no additives, one with 2 wt% UVA, one with 3 wt% HALS, and one with 2 wt% UVA + 3 wt% HALS. The accumulation of CDP in the two HALS-containing films was significantly slower compared to the two films without HALS, clearly demonstrating the degradation suppression capability of HALS. On the other hand, UVA did not slow down the degradation rate, even though it is commonly used as a stabilizer in polyurethane. This raises the question: why is UVA empirically considered useful and commonly added to protective polyurethane layers? It can be inferred that while UVA does not suppress the degradation of the protective layer itself, it may reduce UV transmittance to underlying layers in practical material design. Another significant finding is that UVA leached out much faster compared to HALS (Fig. 4C, blue vs Fig. 4D, orange). However, in the system where both HALS and UVA were added (Fig. 4D, teal), the leaching of UVA was suppressed, likely because HALS slowed the degradation of the matrix polymer. This suggests that the leaching of stabilizers is primarily driven by matrix polymer degradation. Since stabilizers like HALS suppress the degradation of the matrix polymer, it can be concluded that degradation and leaching are complementary processes. The degradation degree defined by NL-RQMS captured both behaviors simultaneously, further demonstrating its usefulness.

3.5. *Correlating the degree of degradation and mechanical property*

By defining the degree of degradation based on the CDP weight fraction, we can now correlate chemical composition with mechanical properties and identify the chemical threshold that induces a mechanical phase shift and the massive dispersal of microplastics [7]. To evaluate the mechanical properties of fragile films, we conducted micro-indentation tests, which assess surface stiffness by measuring the indentation depth at a fixed applied force [20]. Fig. 5 represents the maximum indentation depth and indentation elastic modulus plotted against the degree of degradation. Since no changes in indentation depth were observed between films with (blue) and without (red) HALS before degradation, the two data sets were combined to represent the full range of degradation, from 0 to 80 %. When the degree of degradation exceeded 50 %, the maximum indentation depth suddenly decreased, indicating a threshold in the chemical composition that triggered sudden mechanical deterioration. This demonstrated that degradation progressed without significant changes in mechanical properties until a critical point was reached, highlighting the importance of monitoring chemical composition to predict sudden failure in advance. The decrease in indentation depth also indicated an increase in surface stiffness (Fig. 5, dashed curve), suggesting that the film surface became harder and more brittle as degradation progressed. To further investigate internal mechanical changes, we performed SAICAS on the same samples used for micro-indentation.

Fig. 6A-B shows the image of the film scraping process by SAICAS. In Stage I, the ceramic knife cut the film at an angle of about 5.7 ^{o} until reaching at 25 mm depth, and then in Stage II, it cut the film horizontally for 1250 mm. During the film scraping process, a horizontal force loaded to the knife was recorded, allowing for the estimation of the stiffness of internal materials. However, no significant changes in horizontal load curves were observed as degradation progressed (Fig. S3), suggesting that evaluating the internal mechanical properties based solely on the absolute values of horizontal load was challenging. Therefore, we focused on the slope of the horizontal load per film width during Stage I and the frequency of horizontal load fluctuations in Stage II (Fig. 6C). Drawing an analogy to the slope of a stress-strain curve (elastic modulus), the slope of the horizontal load per film width as a function of the knife's scanning distance represents the stiffness of the material, which we refer to as apparent shear stiffness [21]. On the other hand, the frequency of load fluctuations during the scanning in Stage II has not been extensively discussed. The periodic response in horizontal load is likely attributable to crock propagation; when the knife moves through voids formed by crack propagation, the horizontal loaded decreases. Since the length scale of crack propagation reflets the interconnected domain size, the frequency analysis of horizontal load in Stage II can reveal the size of the mechanically interconnected domains.

For apparent shear stiffness analysis, a stable load response cannot be obtained in shallow regions due to the surface roughness. Therefore, it is common to perform linear fitting in the deeper regions beyond the breakpoint marked as star in Fig. 6C. The representative load curves before and after degradation without additives are presented in Fig. 6C. The measurements were conducted four times for each film. The resulting apparent shear stiffness for films with and without HALS at different degrees of degradation is shown in Fig. 6D. An inflection point was observed around degradation degree of 0.5, indicating that not only the surface but also the interior of films suddenly becomes harder when

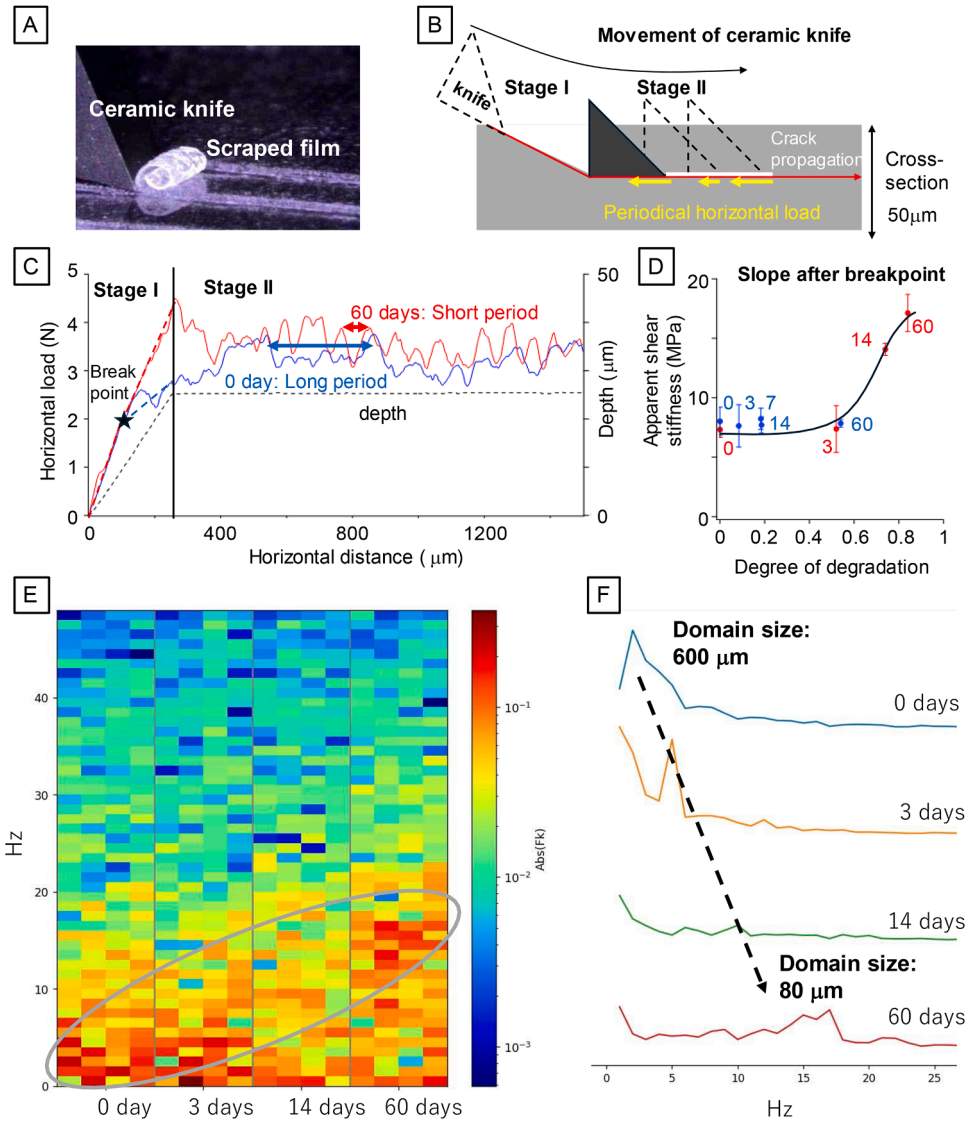

Fig. 6. SAICAS analysis. (A-B) Image of the film scraping process. (C) Representative horizontal load curves before (blue) and after (red) degradation. (D) Slopes in Stage I after the breakpoint plotted as a function of the degree of degradation. The blue and red dots represent the average slopes for four iterations for films containing HALS (blue) or no stabilizers (red). Error bars represent the standard deviation for the four trials. (E) Discrete Fourier Transform (DFT) analysis of horizontal load for films without stabilizers. The gray circle indicates the frequency shift with degradation progression, visualizing all four trials. (F) Frequency distribution averaged over the four trials.

the accumulation of degradation products exceeds 50 %.

The frequency analysis of Stage II for the non-additive system is presented in Fig. 6E. As degradation progresses, strong signals appeared at higher frequencies. The average frequency distribution over four trials is shown in Fig. 6F. The peak shift from lower to higher frequencies indicated a decrease in the interconnected domain size from 600 to 80 μm. Combining these mechanical evaluations, we concluded that the accumulation of degraded products suddenly made the entire material harder and more brittle. The degree of degradation defined by CDP fraction can predict these sudden changes in advance.

In this paper, we introduced a novel metric for assessing polymer degradation, defined by the CDP weight fraction. Polymer materials undergo various forms of degradation depending on their chemical structure, stabilizers, and environmental conditions, making it challenging to fully understand all degradation pathways—particularly when chemical composition details are unavailable. However, by leveraging spectral variations in pyrolysis-MS caused by degradation and applying the NL-RQMS algorithm, we demonstrated that the degree of degradation can be quantitatively determined without requiring prior knowledge of the system. By correlating changes in mechanical properties with this defined degradation degree, we identified the threshold at which a mechanical phase shift occurs, signaling the material's end-of-life. Identifying such thresholds is critical for developing strategies to prevent sudden infrastructure failures and mitigate the environmental impact of microplastic release and additive leaching. Moreover, tracking the chemical degradation degree has proven effective in deriving guidelines for developing degradation-resistant materials, as it revealed that polymer degradation and stabilizer leaching are complementary processes, while also enabling a comparison of different stabilizers' performance. Additionally, the quantitative evaluation of both degradation and residual stabilizers holds great potential for grading recycled materials. However, it should be noted that the proposed CDP-based approach cannot account for mechanical degradation accompanied by material loss, such as surface peeling, erosion by water or sand, or microplastic formation, if the missing material is not present in the analyzed sample. To address this, complementary techniques—such as mass loss measurements, microplastic spectroscopic imaging, and scanning electron microscopy for surface morphology analysis—would

be necessary in environments where physical factors play a significant role [27]. This comprehensive degradation metric, based on pyrolysis-MS and surpassing the conventional carbonyl index in both scope and precision, could play a pivotal role in advancing a sustainable coexistence with plastics.

CRediT authorship contribution statement

Yusuke Hibi: Writing – review & editing, Writing – original draft, Visualization, Validation, Supervision, Software, Project administration, Funding acquisition, Formal analysis, Data curation, Conceptualization. **Tsukasa Matsumoto:** Investigation. **Masatoshi Midorikawa:** Investigation. **Shiho Uesaka:** Investigation. **Makoto Mizoshiri:** Investigation. **Toshiyuki Tanimura:** Supervision. **Masato Okada:** Supervision. **Kimiyoshi Naito:** Supervision. **Masanobu Naito:** Supervision, Funding acquisition.

Declaration of competing interest

The authors declare the following financial interests/personal relationships which may be considered as potential competing interests:

Yusuke Hibi reports financial support was provided by Japan Society for the Promotion of Science. Masanobu Naito reports financial support was provided by Japan Science and Technology Agency. Masanobu Naito reports financial support was provided by Government of Japan Ministry of Education Culture Sports Science and Technology. If there are other authors, they declare that they have no known competing financial interests or personal relationships that could have appeared to influence the work reported in this paper.

Acknowledgements

This work was supported by JSPS KAKENHI Grant Number JP24K08520 (to Y.H.), Core Research for Evolutional Science and Technology program of Japan Science and Technology Agency under Grant JPMJCR19J3 and MEXT Program: Data Creation and Utilization-Type Material Research and Development Project Grant Number JPMXP1122714694 (to M.N.).

Supplementary materials

Supplementary material associated with this article can be found, in the online version, at doi:10.1016/j.polymdegradstab.2024.111128.

Data availability

All data utilized in this study are included in the supplementary materials.

References

[1] J. Xie, Y. Yan, S. Fan, X. Min, L. Wang, X. You, X. Jia, G.I.N. Waterhouse, J. Wang, J. Xu, Prediction model of photodegradation for PBAT/PLA mulch films: strategy to fast evaluate service life, Environ. Sci. Technol 56 (12) (2022) 9041–9051.
[2] I. Oluwoye, L.L. Machuca, S. Higgins, S. Suh, T.S. Galloway, P. Halley, S. Tanaka, M. Iannuzzi, Degradation and lifetime prediction of plastics in subsea and offshore infrastructures, Sci. Total Environ. 904 (2023) 166719.
[3] A. Chamas, H. Moon, J. Zheng, Y. Qiu, T. Tabassum, J.H. Jang, M. Abu-Omar, S. L. Scott, S. Suh, Degradation rates of plastics in the environment, ACS Sustain. Chem. Eng. 8 (2020) 3494–3511. *ACS Sustain. Chem. Eng.* **2020**, *8* (9), 3494–3511.
[4] S.S. Ali, T. Elsamahy, E. Koutra, M. Kornaros, M. El-Sheekh, E.A. Abdelkarim, D. Zhu, J. Sun, Degradation of conventional plastic wastes in the environment: a review on current status of knowledge and future perspectives of disposal, Sci. Total Environ. 771 (2021) 144719.
[5] Y. Li, Y. Liu, S. Liu, L. Zhang, H. Shao, X. Wang, W. Zhang, Photoaging of baby bottle-derived polyethersulfone and polyphenylsulfone microplastics and the resulting bisphenol S release, Environ. Sci. Technol 56 (5) (2022) 3033–3044.
[6] Y. Zhang, Y. Peng, C. Peng, P. Wang, Y. Lu, X. He, L. Wang, Comparison of detection methods of microplastics in landfill mineralized refuse and selection of degradation degree indexes, Environ. Sci. Technol. 55 (20) (2021) 13802–13811.
[7] E. Syranidou, K. Karkanorachaki, D. Barouta, E. Papadaki, D. Moschovas, A. Avgeropoulos, N. Kalogerakis, Relationship between the Carbonyl Index (CI) and Fragmentation of Polyolefin plastics during aging, Environ. Sci. Technol 57 (21) (2023) 8130–8138.
[8] H.H. Chin, P.S. Varbanov, F. You, F. Sher, J.J. Klemeš, Plastic circular economy framework using hybrid machine learning and pinch analysis, Resour. Conserv. Recycl. 184 (2022) 106387.
[9] J.P. Lange, Managing plastic waste-sorting, recycling, disposal, and product redesign, ACS Sustain. Chem. Eng 9 (47) (2021) 15722–15738.
[10] polymer degradation, The IUPAC Compendium of Chemical Terminology, International Union of Pure and Applied Chemistry (IUPAC), 2008, https://doi.org/10.1351/goldbook.pt07144.
[11] R.S. Gomes, A.N. Fernandes, W.R. Waldman, How to measure polymer degradation? an analysis of authors' choices when calculating the carbonyl index, Environ. Sci. Technol. 58 (17) (2024) 7609–7616.
[12] N. Kasyapi, R. Mehta, A.K. Bhowmick, Raman and NMR spectroscopic studies on hydrolytic degradation of D,L-Lactide - δ-Valerolactone - D,L-Lactide Copolymer, ACS Sustain. Chem. Eng. 3 (7) (2015) 1381–1393.
[13] M.R. Salazar, J.D. Kress, J.M. Lightfoot, B.G. Russell, W.A. Rodin, L. Woods, Low-temperature oxidative degradation of PBX 9501 and its components determined via molecular weight analysis of the Poly[ester urethane] binder, Polym. Degrad. Stab. 94 (12) (2009) 2231–2240.
[14] F. Awaja, P.J. Pigram, Surface molecular characterisation of different epoxy resin composites subjected to UV accelerated degradation using XPS and ToF-SIMS, Polym. Degrad. Stab. 94 (4) (2009) 651–658.
[15] Y. Hibi, S. Uesaka, M. Naito, A data-driven sequencer that unveils latent "codons" in synthetic copolymers, Chem. Sci. 14 (2023) 5619–5626.
[16] Y. Hibi, S. Uesaka, M. Naito, Thermogravimetry-synchronized, reference-free quantitative mass spectrometry for accurate compositional analysis of polymer systems without prior knowledge of constituents, Analyst 149 (2024) 4388–4394.
[17] Y. Hibi, Reference-free quantitative mass spectrometry in the presence of nonlinear distortion caused by in situ chemical reactions among constituents, Analyst 149 (2024) 5320–5328.
[18] S. Wei, V. Pintus, M. Schreiner, Photochemical degradation study of polyvinyl acetate paints used in artworks by Py–GC/MS, J. Anal. Appl. Pyrolysis 97 (2012) 158–163.
[19] M. Ogata, Y. Mochizuki, M. Furuya, A. Terasawa, N. Katsumata, Correlation Between the Degree of Deterioration by Accelerated Weathering Apparatus and By Outdoor Exposure—In Case Evaluating Deterioration of Polypropylene—, 36, Seikei-Kakou, 2024, pp. 299–305.
[20] K. Shirasu, K. Goto, K. Naito, Microstructure-elastic property relationships in carbon fibers: a nanoindentation study, Compos. B Eng. 200 (2020) 108342.
[21] E. Kim, H. Yun, J. Lee, W.E. Lee, K. Heo, I.H. Jung, I.Y. Song, Evaluation method for microscale mechanical properties of an epoxy resin, Polym. Test 135 (2024) 108458.
[22] Y. Hibi, Y. Tsuyuki, S. Ishii, E. Ide, M. Naito, Decoding thermal properties in polymer-inorganic heat dissipators: a data-driven approach using pyrolysis mass spectrometry, Sci. Technol. Adv. Mater. 25 (1) (2024) 2362125, https://doi.org/10.1080/14686996.2024.2362125.
[23] R. Watanabe, S. Nakamura, A. Sugahara, M. Kishi, H. Sato, H. Hagihara, H. Shinzawa, Revealing molecular-scale structural changes in polymer nanocomposites during thermo-oxidative degradation using evolved gas analysis with high-resolution time-of-flight mass spectrometry combined with principal component analysis and kendrick mass defect analysis, Anal. Chem. 96 (6) (2024) 2628–2636.
[24] S. Yamane, S. Nakamura, R. Inoue, T.N.J. Fouquet, T. Satoh, K. Kinoshita, H. Sato, Determination of the block sequence of linear triblock copolyethers using thermal desorption/pyrolysis direct analysis in real-time mass spectrometry, Macromolecules 54 (22) (2021) 10388–10394.
[25] I.J. Gomez, J. Wu, J. Roper, H. Beckham, J.C. Meredith, High throughput screening of mechanical properties and scratch resistance of tricomponent polyurethane coatings, ACS Appl. Polym. Mater. 1 (11) (2019) 3064–3073, https://doi.org/10.1021/ACSAPM.9B00726/SUPPL_FILE/AP9B00726_SI_001.PDF.
[26] J.M. Cuevas, R. Cobos, L. Germán, B. Sierra, J.M. Laza, J.L. Vilas-Vilela, Enhanced mar/scratch resistance in automotive clear coatings by modifying crosslinked polyurethane network with branched flexible oligomers, Prog. Org. Coat. 163 (2022) 106668.
[27] A. Al-Darraji, I. Oluwoye, C. Lagat, S. Tanaka, A. Barifcani, Erosion of rigid plastics in turbid (sandy) water: quantitative assessment for marine environments and formation of microplastics, Environ. Sci. Process Impacts 26 (2024) 1847–1858.